J|A|C|S COMMUNICATIONS

Published on Web 04/22/2010

1D $Cu(OH)_2$ Nanomaterial Synthesis Templated in Water Microdroplets

Gilles R. Bourret and R. Bruce Lennox*

Department of Chemistry, McGill University and Center for Self-Assembled Chemical Structure (CSACS), 801 Sherbrooke Street West, Montreal, Quebec, H3A 2K6, Canada

Received February 23, 2010; E-mail: bruce.lennox@mcgill.ca

The hierarchical assembly of nanomaterials creates many opportunities for the spontaneous formation of structures.[1] For many applications, micro- and nanostructured materials show a strong correlation between their geometry and their function.[2] Catalytic, sensing, or photovoltaic activity often depends on the effective surface area, making porous and hollow materials excellent candidates for these applications. Controlled hollow material synthesis strategies include hard templating, sacrificial templating, soft templating, and template-free methods.[1b,2] Soft templating is a particularly attractive technique due its modulability, flexibility, and simplicity. Emulsions are a good example of soft templates and have been shown to be efficient in polymer particle[2,3] and porous material[4] fabrication. They have, for example, been used to make TiO_2 and SiO_2 hollow structures through sol−gel processes. However, their application has often been restricted to the use of reactive metal alkoxides.[5]

Mesoscale organization of metal oxide materials has been of considerable interest given the current understanding of nonclassical crystallization processes. For example, the aqueous assembly of CuO nanoribbons into "dandelions" due to geometrical constraints, has recently been reported.[6] Similarly the crystallization of ZnO via a local dipolar electric field has been recently demonstrated.[7] Among the large number of metal oxide nanostructures that can be synthesized, copper oxide is particularly important given its low cost and its use as a p-type semiconductor in lithium-ion batteries,[8] and photovoltaic,[9] photocatalytic,[10] and sensing[11] applications. Template-free syntheses of $Cu(OH)_2$ and CuO of various shapes (microparticles, nanoribbons, nanowires) have been reported,[12,13] while copper oxalate precipitation was recently templated using a microemulsion to produce solid CuO microspheres via thermolysis.[14]

In this Communication we report the interfacial synthesis of copper hydroxide nanofibers (NF) in a two-phase system (H_2O/CH_2Cl_2) that subsequently self-assemble to form porous microbeads. We show that this mesoscale aggregation process is driven by the water-in-oil (W/O) emulsion templating the formation of the NF. The NF formed at the H_2O/CH_2Cl_2 interface adsorb on the water droplet surface leading to spherical networks of copper hydroxide NF (Scheme 1). Thermolysis leads to novel photoresponsive porous CuO beads.

Reactions were conducted in 8 dram vials (Fisherbrand) using a 1 cm stirring bar (Fisherbrand) under vigorous stirring (900 rpm). In a typical synthesis, 0.4 mM of $CuCl_2 \cdot 2H_2O$ (Sigma, 99%) is dissolved in 5 mL of CH_2Cl_2 with 5 equiv of *n*-butylamine (Sigma, 99.5%), forming a blue copper−amine complex. Alkylamines solubilize metal salts in organic solvents through coordination with the metal cations[15] and can form CuX_2[alkylamine]$_2$ complexes with copper(II) salts.[16] Upon addition of 5 mL of Milli-Q water, the organic phase immediately becomes cloudy blue-green. The pH of the aqueous phase increases to 10 due to the high concentration of butylamine (butylamine $pK_a = 10.6$),[17] causing the copper−amine complex to rapidly precipitate at the H_2O/CH_2Cl_2 interface. Copper

Scheme 1. $CuCl_2$−Butylamine Complex Precipitation at the Water Droplet Surface and Anisotropic Growth of $Cu(OH)_2$

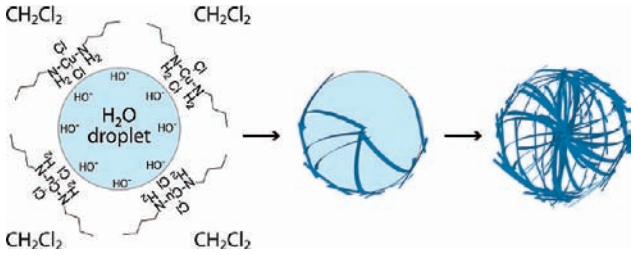

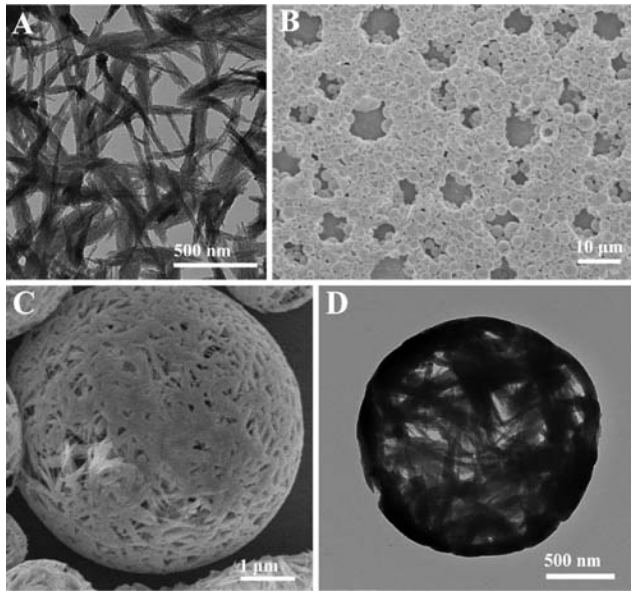

Figure 1. (A) TEM image of the $Cu(OH)_2$ NF **1b** present at the early stage of the reaction. (B,C) SEM and (D) TEM of the resulting microspheres **2a** composed of **1b**.

hydroxide NF form in both phases (Figure 1, Supporting Information(SI)) at this stage (referred to as **1a** for the H_2O phase and to **1b** for the cloudy CH_2Cl_2 phase). Rapid isolation and filtration (within 10 min) of both phases after 5 min of reaction through a polyvinylidene fluoride membrane (0.2 μm, Pall FP Vericel 200) and washing (**1a** with H_2O and **1b** with CH_2Cl_2) lead to isolation of pure $Cu(OH)_2$ NF. Fibers formed in water are 12.0 ± 3.7 nm wide on average and >1 μm long. Those present in the organic phase are shorter (average width of 14.5 ± 4.2 nm and length of 500 ± 217 nm) and have a pronounced curved shape. When the reaction is allowed to proceed to completion (35 min), the organic phase settles in 1 h in a separatory funnel and is isolated. Careful successive washing/precipitation steps (using CH_2Cl_2) were conducted over a period of 24 h followed by membrane filtration and vacuum drying. A powdery blue material, revealed by electron

microscopy to be porous microspheres (named **2a**) composed of **1b**, is isolated. As seen in Figure 1B, the vast majority of the NF are present as spherical aggregates. Copper,[18a] zinc,[18b] and cadmium[18c] salts are known to form hydroxide NF in aqueous solutions under specific conditions. Recently $Cd(OH)_2$ nanowires were found to slowly grow at a quiescent toluene−water interface.[18d] These precedents suggest that similar processes occur in this $Cu(OH)_2$ system and are consistent with the interfacial precipitation of the copper−butylamine complex as $Cu(OH)_2$ NF. Optical microscopy (SI) suggests that a microemulsion rapidly forms in the CH_2Cl_2 phase (within 30 s after the water addition). The microemulsion does not form if $CuCl_2 \cdot 2H_2O$ is absent. Although a Pickering emulsion[19] (i.e., an emulsion stabilized by solid particles) might have formed, the absence of spheres at the early stages of the reaction suggests that this is not the case. After 30 s, only a very small quantity of NF is apparent. It is likely that the copper butylamine complex stabilizes the water droplet by acting as a surfactant. An emulsion in fact occurs when the butylamine is present in as low as 2 equiv. The curved shape of the fibers (Figure 1A) formed in the opaque CH_2Cl_2 phase after 5 min of stirring (**1b**) is consistent with copper precipitation at the water droplet surface. Geometric analysis of the fiber curvature (SI) yields a mean diameter of curvature of 1.61 μm (standard error 0.15 μm), consistent with the range of the H_2O droplet diameters measured with optical microscopy (1.8 μm after 5 min of stirring). The smoothness and the evident filling of the spheres (Figure 1C and 1D) are further evidence that the precipitation at the microdroplet surface determines the resulting material morphology. The late appearance of the spheres in the reaction mixture results from the slow growth of the NF from the water droplet surface into its interior, which is limited by the generation and the diffusion of the reactants (Cu^{2+}, OH^-, and Cl^-) into the aqueous phase. This growth process is clearly different from the classically described precipitation at the droplet surface, as per that involved in emulsion-based hollow materials.[1b,2]

Both the size (Figure 2) and the morphology (Figure 3) of the resulting structures were successfully altered by adding a short chain alcohol (*n*-butanol, Sigma, HPLC grade) to the CH_2Cl_2 phase prior to the water addition (Scheme 2). At 2 vol% and 4.5 vol% butanol, porous spheres made of long fibers and short ribbons are obtained. The sphere size (ca. 2.5 μm without butanol) increases to 3 μm (**3**, 2 vol% butanol) and to 3.8 μm (**4**, 4.5 vol% butanol). At 9 and 16.5 butanol vol%, completely hollow spheres made of self-assembled short nanoribbons form (referred to as **5** and **6a**). The sphere diameter increases to 4.5 and 5 μm, respectively, in these cases. The color of the different products depends on their morphology. Blue products (attributed to $Cu(OH)_2$) arise in the absence of butanol and become green jade (characteristic of copper hydroxychloride) as butanol is added. Products were characterized with powder X-ray diffraction (XRD), Fourier transform infrared (FTIR), thermogravimetric (TGA), energy-dispersive X-ray (EDS), and UV−vis diffuse reflectance analyses. XRD and FTIR analyses confirm that **2a**, **3**, and **4** are composed of $Cu(OH)_2$ (PDF 13-0420) and copper hydroxychloride (mixture of two polymorphs: atacamite, PDF 78-0372 and clinoatacamite),[20] while the samples made via a greater butanol content (**5** and **6a**) are pure copper hydroxychloride. FTIR spectra show the progressive disappearance of the intense band around 700 cm^{-1} characteristic of pure $Cu(OH)_2$[21] as the butanol content increases (SI). The NF formed at the beginning of the reaction without butanol (**1a** and **1b**) are composed of pure $Cu(OH)_2$ (SI). Butanol allows for a fine-tuning of the size and the morphology at both the meso- and the nanoscale by suppressing the anisotropic precipitation of the copper−butylamine complex

Scheme 2. Schematic Sectional View of the Different Morphologies and Sizes As a Function of the Butanol Volume Used in the Synthesis[a]

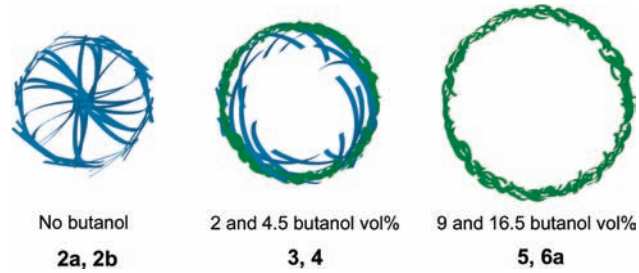

[a] Blue implies $Cu(OH)_2$, and green implies $Cu_2(OH)_3Cl$.

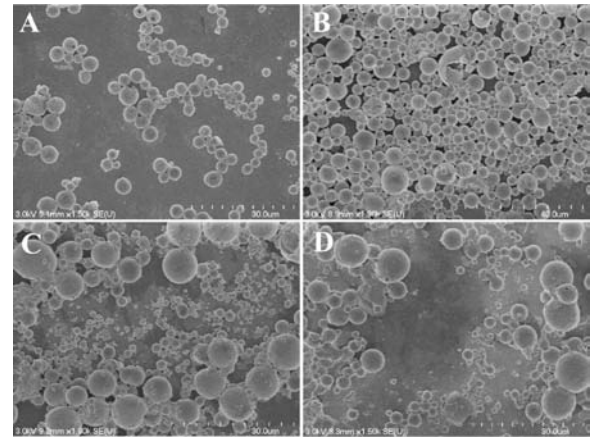

Figure 2. Large scale SEM images of the microspheres obtained when butanol is added to the reaction mixture. (A) **3**, 2 vol%; (B) **4**, 4.5 vol%; (C) **5**, 9 vol%; (D) **6a**, 16.5 vol%.

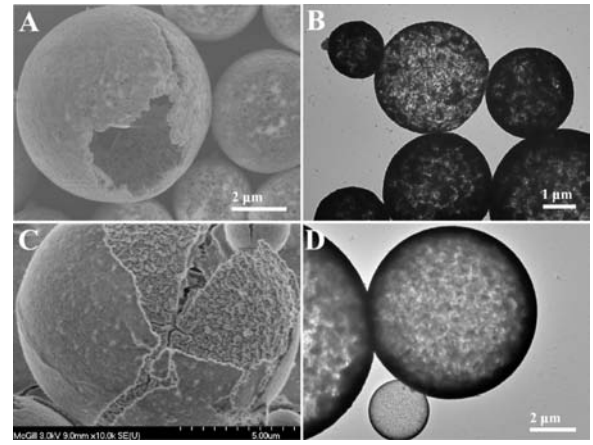

Figure 3. SEM and TEM images of the internal morphologies of the spheres formed, as a function of the amount of butanol added to the reaction. (A) SEM and (B) TEM images of **4** (4.5 butanol vol%). (C) SEM and (D) TEM images of **5** (9 butanol vol%).

at the water droplet surface. Since $Cu(OH)_2$ is known to spontaneously form 1D nanostructures in water,[18a] we propose that butanol selectively alters the interfacial reaction conditions by preferentially driving the precipitation of $Cu_2(OH)_3Cl$ over $Cu(OH)_2$ in the vicinity of the water droplet surface. The precipitation of these two copper hydroxide salts depends on the relative concentration of Cl^- and OH^-, and added butanol will modify this equilibrium. We investigated the influence of OH^- concentration by using a basic aqueous stock solution (0.01 M NaOH) in the reaction instead of neutral pure water without butanol (**2b**) and with 16.5 butanol vol%

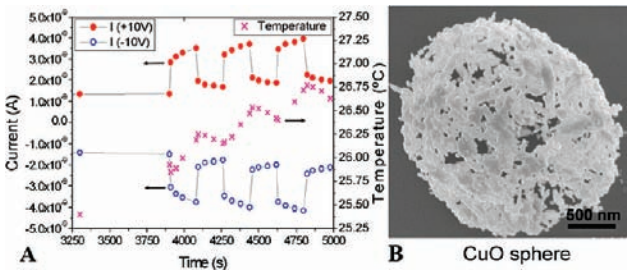

Figure 4. (A) Time evolution of the current measured at +10 V and −10 V applied bias (left axis) and the corresponding temperature of the sample holder (right axis). We verified that the temperature changes were not causing the large current variations observed (SI). Lines are a guide to the eyes. (B) SEM image of **2a** thermolyzed at 500 °C for 3 h.

(**6b**). Without butanol, the morphology does not change (SI). With 16.5 butanol vol%, the hollow spheres form from a mixture of fibers and particles (SI), consistent with the anisotropic fibers being composed of $Cu(OH)_2$.

Thermolysis of these microstructures (in ambient atmosphere) leads to CuO[22] porous microbeads (Figure 4) containing residual Cu_2O (3 h at 500 °C) and pure CuO (15 h at 600 °C). These resulting CuO spheres are photoresponsive upon formation of a metal/semiconductor/metal junction. CuO spheres dispersed in H_2O were drop-cast onto commercial gold microelectrodes (100 nm thick, 15 μm wide and 15 μm spaced) deposited on glass (IAME 1504.3 from Abtech Scientific, Virginia) followed by overnight drying in a vacuum oven. To avoid any contribution from oxygen[23] we performed the electrical characterization of the device under vacuum (10^{-6} mbar). The light source irradiance was 10.7 $mW \cdot cm^{-2}$, and the emission was restricted to the visible region (350−750 nm). IV curves of the device (SI) show a significant increase in the current upon light illumination due to the photogeneration of electrical carriers. The ratio $(I_{light} - I_{dark})/I_{dark} = I_{photo}/I_{dark}$ reaches 2.22 at +10 V bias (2.27 at −10 V) after 180 s of illumination (Figure 4). We note a small irreversibility (10%) upon recovery of the dark current, probably due to a local thermal increase of the CuO spheres (SI). We are not aware of prior reports regarding CuO nanostructure light sensors, and the high I_{photo}/I_{dark} ratio of our device makes it competitive when compared with recent results on Cu_2O nanowires (I_{photo}/I_{dark} of ∼1 at +10 V bias).[11c]

To our knowledge, this is the first demonstration of the *in situ* synthesis of 1D nanostructures that self-assemble at both the surface and the inside of microemulsion droplets. Although anisotropic particles have been used as efficient stabilizers for Pickering emulsions,[24] the relative surface tensions of the two liquid phases and the particle defines the equilibrium location of the particle, restricted to the droplet surface.[19] Cross-linking of the resulting structures often requires an additional polymerization step,[25] that might alter the catalytic and electronic properties of these materials. Hollow ordered assemblies (spheres, tubes) have been prepared from metal−polypyrrole nanorods that self-aggregate and form the structure shells.[26] This method however requires a complex process (successive electrodeposition steps in a porous alumina template) and highly monodisperse nanorods.

The preparation technique reported here is rapid (less than 1 h) and benefits from the simplicity and the tunability of emulsions. Preliminary experiments to make similar $Zn(OH)_2$ and $Cd(OH)_2$ structures, known to form comparable fibers,[18b,c] have not been successful to date. However, alternative pathways are being explored, and we anticipate being able to create new precursors of these technologically important luminescent oxides. Facile control over the structure size (from 2.5 to 5 μm) and morphology is achieved at both the mesoscale (completely hollow versus porous) and the nanoscale (nanoribbons versus nanofibers) by the addition of a short chain alcohol. The selective precipitation of $Cu_2(OH)_3Cl$ over $Cu(OH)_2$ by changing the solvent composition opens new paths for emulsion-based syntheses and interfacial reactions. Finally, the transformation of these materials into porous CuO spheres has several potential applications, including demonstrated intense response to visible light. The high surface area of these hollow microstructures makes them also particularly good candidates for use in catalytic and photocatalytic processes. We expect that this self-assembly strategy will have a strong impact on the manipulation of 1D nanostructures and the fabrication of hollow metal oxide materials.

Acknowledgment. The authors thank the Natural Sciences and Engineering Research Council of Canada and the Center for Self-Assembled Chemical Structures for their financial support.

Supporting Information Available: TGA, IR, EDS, and XRD analyses; SEM and TEM images; experimental protocols; size distributions; and summary tables. This material is available free of charge via the Internet at http://pubs.acs.org.

References

(1) (a) Mann, S. *Nat. Mater.* **2009**, *8*, 781–792. (b) Meldrum, F. C.; Colfen, H. *Chem. Rev.* **2008**, *108*, 4332–4432. (c) Zhang, Q.; Liu, S.-J.; Yu, S.-H. *J. Mater. Chem.* **2009**, *19*, 191–207.
(2) Lou, X. W.; Archer, L. A.; Yang, Z. *Adv. Mater.* **2008**, *20*, 3987–4019.
(3) *Polymer Particles*; Okubo, M., Ed.; Advances in Polymer Science Series *175*; Springer: Berlin, 2005.
(4) Imhof, A.; Pine, D. J. *Nature* **1997**, *389*, 948–951.
(5) (a) Li, W.; Sha, X.; Dong, W.; Wang, Z. *Chem. Commun.* **2002**, 2434–2435. (b) Collins, A. M.; Spickermann, C.; Mann, S. *J. Mater. Chem.* **2003**, *13*, 1112–1114.
(6) Liu, B.; Zeng, H. C. *J. Am. Chem. Soc.* **2004**, *126*, 8124–8125.
(7) Liu, Z.; Wen, X. D.; Wu, X. L.; Gao, Y. J.; Chen, H. T.; Zhu, J.; Chu, P. K. *J. Am. Chem. Soc.* **2009**, *131*, 9405–9412.
(8) Park, J. C.; Kim, J.; Kwon, H.; Song, H. *Adv. Mater.* **2009**, *21*, 803–807.
(9) Mittiga, A.; Salza, E.; Sarto, F.; Tucci, M.; Vasanthi, R. *Appl. Phys. Lett.* **2006**, *88*, 163502.
(10) Hara, M.; Kondo, T.; Komoda, M.; Ikeda, S.; Shinohara, K.; Tanaka, A.; Kondo, J. N.; Domen, K. *Chem. Commun.* **1998**, 357–358.
(11) (a) Zhang, J.; Liu, J.; Peng, Q.; Wang, X.; Li, Y. *Chem. Mater.* **2006**, *18*, 867–871. (b) Zhang, H.; Zhu, Q.; Zhang, Y.; Wang, Y.; Zhao, L.; Yu, B. *Adv. Funct. Mater.* **2007**, *17*, 2766–2771. (c) Sahoo, S.; Husale, S.; Colwill, B.; Lu, T.-M.; Nayak, S.; Ajayan, P. M. *ACS Nano* **2009**, *3*, 3935–3944.
(12) Durand-Keklikian, L.; Matijevic, E. *Colloid Polym. Sci.* **1990**, *268*, 1151–8.
(13) (a) Lu, C.; Qi, L.; Yang, J.; Zhang, D.; Wu, N.; Ma, J. *J. Phys. Chem. B* **2004**, *108*, 17825–17831. (b) Wen, X.; Xie, Y.; Choi Chun, L.; Wan Kwun, C.; Li, X.-Y.; Yang, S. *Langmuir* **2005**, *21*, 4729–37. (c) Zhong, Z.; Ng, V.; Luo, J.; Teh, S.-P.; Teo, J.; Gedanken, A. *Langmuir* **2007**, *23*, 5971–7. (d) Wang, H.; Shen, Q.; Li, X.; Liu, F. *Langmuir* **2009**, *25*, 3152–3158.
(14) He, Y. *Mater. Res. Bull.* **2007**, *42*, 190–195.
(15) Yang, J.; Ying, J. Y. *Nat. Mater.* **2009**, *8*, 683–689.
(16) Busico, V.; Carfagna, C.; Salerno, V.; Vacatello, M. *Thermochim. Acta* **1980**, *39*, 1–5.
(17) Lide, D. R., Ed. *CRC Handbook of Chemistry and Physics*, 90th ed.; CRC Press: 2010.
(18) (a) Luo, Y.-H.; Huang, J.; Jin, J.; Peng, X.; Schmitt, W.; Ichinose, I. *Chem. Mater.* **2006**, *18*, 1795–1802. (b) Peng, X.; Jin, J.; Kobayashi, N.; Schmitt, W.; Ichinose, I. *Chem. Commun.* **2008**, 1904–1906. (c) Ichinose, I.; Kurashima, K.; Kunitake, T. *J. Am. Chem. Soc.* **2004**, *126*, 7162–7163. (d) Mlondo, S. N.; Andrews, E. M.; Thomas, P. J.; O'Brien, P. *Chem. Commun.* **2008**, 2768–2770.
(19) Hunter, T. N.; Pugh, R. J.; Franks, G. V.; Jameson, G. J. *Adv. Colloid Interface Sci.* **2008**, *137*, 57–80.
(20) Jambor, J. L.; Dutrizac, J. E.; Roberts, A. C.; Grice, J. D.; Szymanski, J. T. *Can. Mineral.* **1996**, *34*, 61–72.
(21) Cabannes-Ott, C. *Comptes rendus* **1956**, *242*, 2825–2827.
(22) (a) Sharkey, J. B.; Lewin, S. Z. *Thermochim. Acta* **1972**, *3*, 189–201. (b) Tanaka, H.; Sadamoto, T. *Thermochim. Acta* **1982**, *54*, 273–280.
(23) Kolmakov, A.; Moskovits, M. *Annu. Rev. Mater. Res.* **2004**, *34*, 151–180.
(24) Madivala, B.; Vandebril, S.; Fransaer, J.; Vermant, J. *Soft Matter* **2009**, *5*, 1717–1727.
(25) Chen, T.; Colver, P. J.; Bon, S. A. F. *Adv. Mater.* **2007**, *19*, 2286–2289.
(26) Park, S.; Lim, J.-H.; Chung, S.-W.; Mirkin, C. A. *Science* **2004**, *303*, 348–341.

JA101579V